Quasiparticles in Photoemission Spectra of Manganites †

Andrzej M. Oleś
Jagellonian University, Cracow, Poland
Max-Planck-Institut FKF, Stuttgart, Germany
(Dresden, 8 April 2005)

† *Dedicated to the memory of John Paul II.*

- Jan Bała, Jagellonian University, Cracow
- Peter Horsch, Max-Planck-Institut FKF, Stuttgart
- George A. Sawatzky, UBC, Vancouver, Canada

1 Orbital t-J model for FM planes:
 — hole dressing by orbiton excitations.

2. Interactions with the lattice:
 — free propagation versus hole confinement;
 — mixed orbiton-phonon excitations.

3. Quantum decoherence in A-AF phase (magnons)

4. 1D orbital t-J model at finite T:
 — from quasiparticles to free propagation.

5. Conclusions — need for ARPES experiments

//www.njp.org

DEUTSCHE PHYSIKALISCHE GESELLSCHAFT | Institute of Physics

Login: Password:
Go

Create account |
Alerts | Contact us

New Journal of Physics
The open-access journal for physics

IOP Journals Home | IOP Journals List | EJs Extra | This Journal | Search | Authors | Referees | Librarians | User Options | Help |
◂ Previous article | Next article ▸ | This volume ▴ | Article options & Content finder ▾

Bernhard Keimer *et al* 2004 *New J. Phys.* **6**

EDITORIAL

Focus on Orbital Physics

The quest for a microscopic understanding of the physical properties of transition metal oxides with orbital degeneracy ('orbital physics') is currently at the forefront of solid-state physics. The field was kicked off nearly 50 years ago by a remarkable pair of papers. In the first, Wollan and Koehler reported using the newly developed technique of neutron scattering to elucidate the lattice and magnetic structures of $La_{2-x}Ca_xMnO_3$ (1955 *Phys. Rev.* **100** 545). This material crystallizes in the perovskite structure, in which each manganese ion is surrounded by an octahedron of six oxygen ions. The MnO_6 octahedra exhibit subtle distortions which lower the lattice symmetry. Wollan and Koehler noticed that the pattern of octahedral distortions varies systematically with Ca content, and that these variations go along with changes in the magnetic ordering pattern of the unpaired 3d electrons on the manganese ions. The basic origin of the lattice superstructure can be readily understood by inspection of the electron configuration of a single Mn^{3+} ion. The cubic crystal field due to the O^2-ligands splits the five 3d levels into a lower-lying, triply degenerate ('t_{2g}') and a higher-lying, doubly degenerate ('e_g') manifold. These levels are filled by the four d-electrons of Mn^{3+} according to Hund's rule, which dictates that three of the four electrons with parallel spins occupy the t_{2g} levels. The orbital degeneracy derives from the remaining electron occupying the e_g manifold. The distortion of the MnO_6 octahedra can be ascribed to a Jahn-Teller distortion that lifts this degeneracy. Since neighbouring octahedra share one oxygen ion, the Jahn-Teller distortion is 'cooperative' and leads to a change in lattice symmetry which favours particular orbitals at neighbouring sites, now referred to as 'orbital ordering'. Different orbital ordering pattern are realized as Ca substitution removes the e_g electron and converts some of the Mn^{3+} ions to orbitally non-degenerate Mn^{4+}.

In the paper immediately following Wollan and Koehler's article, John Goodenough proposed a model describing the interplay between orbital and magnetic superstructures in the manganites (1955 *Phys. Rev.* **100** 564). Briefly, the model predicts that relative orientation of e_g orbitals on neighbouring Mn sites determines the magnitude and sign of the magnetic exchange interactions, which in turn determine the magnetic ordering pattern. Goodenough's model, together with concurrent work by Kanamori and Anderson, led to a detailed understanding of the magnetic interactions and their dependence on orbital occupation, establishing a framework now known as

Observation of orbital waves

LaMnO$_3$

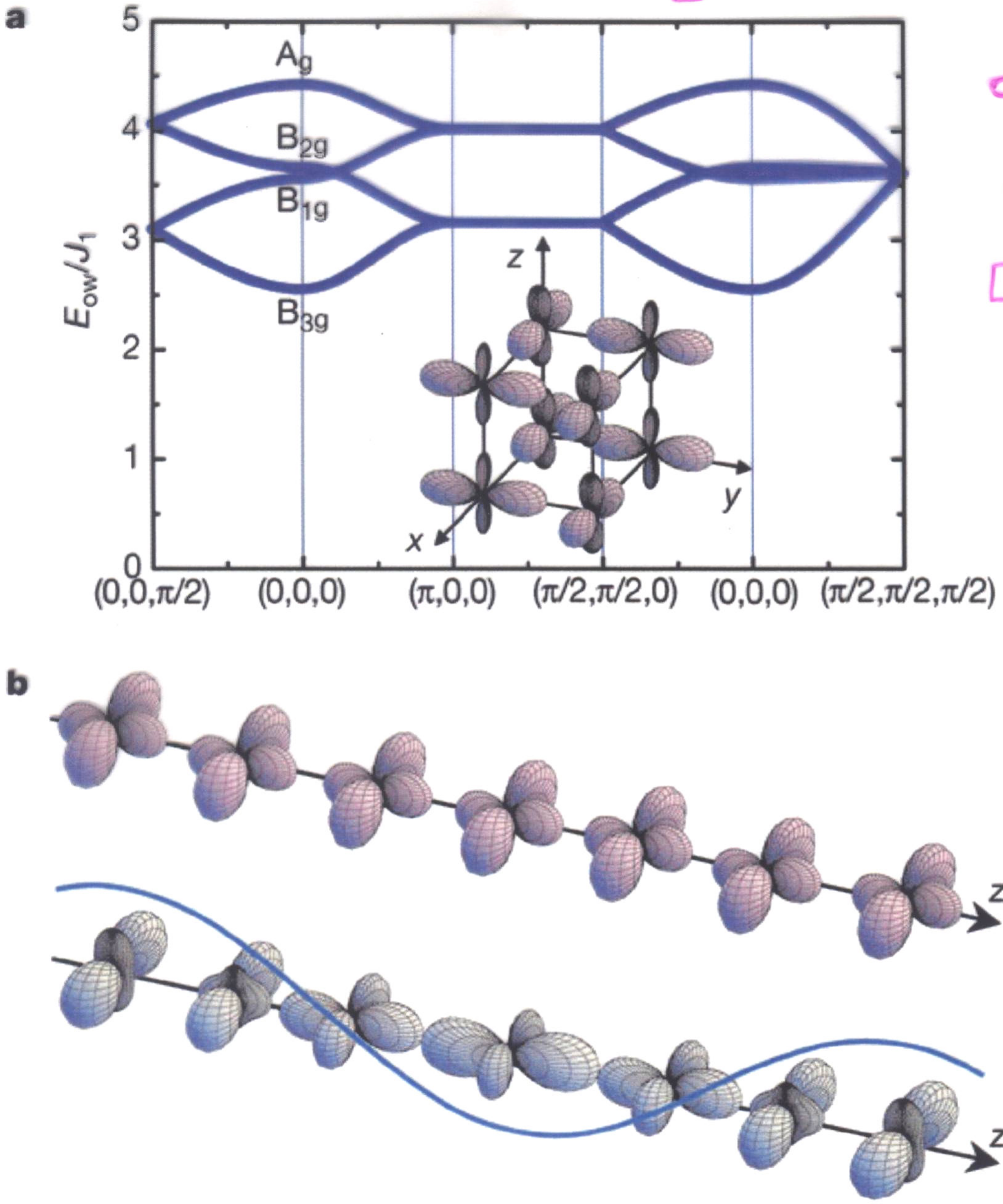

orbitons:

$\omega_q \simeq 3J$

[J. van den Brink et al., PRB (1999)]

ground state

orbital excitation

E. Saitoh et al., Nature 410, 180 (2001)

R. Kilian and G. Khaliullin,

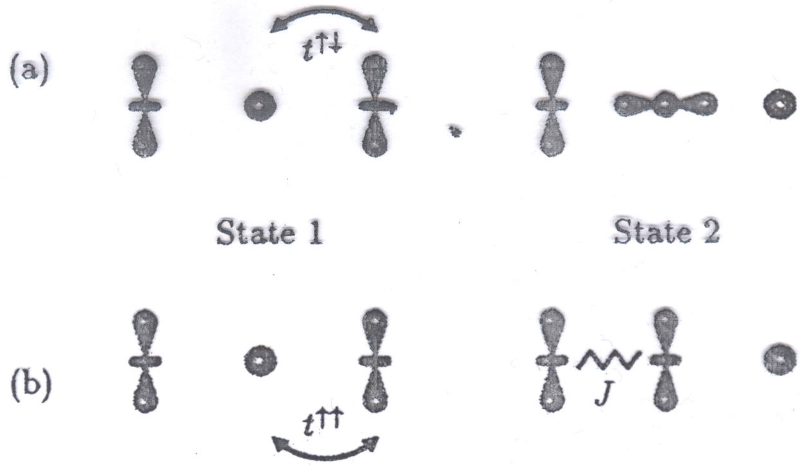

FIG. 1. Coherent (a) and incoherent (b) hole motion in antiferrotype orbital order. Incoherent processes involve the creation of an orbital excitation of energy J.

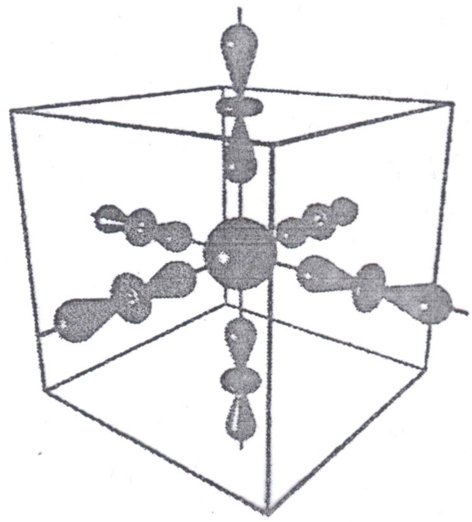

FIG. 5. Orbital polaron in the strong-coupling limit: Six e_g states point towards a central hole.

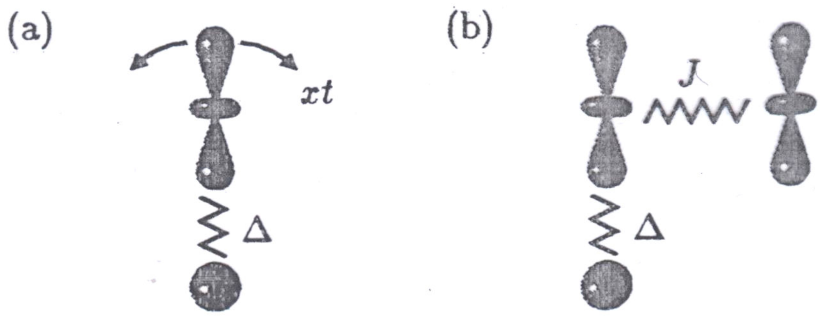

FIG. 6. (a) Orbital fluctuations with an energy scale $\propto xt$ and (b) intersite correlations $\propto J$ compete against the orbital-hole binding energy Δ.

Orbital t-J Model

- **t-J model for e_g electrons in FM planes:**

$$\mathcal{H}_0 = H_t + H_J + H_{\mathrm{JT}} + H_z, \tag{1}$$

Standard orbital basis $\{x^2 - y^2, 3z^2 - r^2\}$ at each site i:

$$|x\rangle \equiv \tfrac{1}{\sqrt{2}}|x^2 - y^2\rangle, \quad |z\rangle \equiv \tfrac{1}{\sqrt{6}}|3z^2 - r^2\rangle. \tag{2}$$

- **The orbital superexchange:**

$$\boxed{H_J = \frac{1}{2}J \sum_{\langle ij\rangle} [T_i^z T_j^z + 3T_i^x T_j^x \mp (T_i^x T_j^z + T_i^z T_j^x)],} \tag{3}$$

$$T_i^z = \tfrac{1}{2}\sigma_i^z = \tfrac{1}{2}(n_{ix} - n_{iz}), \quad T_i^x = \tfrac{1}{2}\sigma_i^x. \tag{4}$$

- **The cooperative JT interaction with the lattice:**

$$\boxed{H_{\mathrm{JT}} = -2\sqrt{6}\lambda \sum_i (Q_{i,2} T_i^x + Q_{i,3} T_i^z),} \tag{5}$$

supports alternating orbitals (minimum obtained with elastic energy $\propto K$ – Mn-O spring constant)

- **Crystal-field term:**

$$\boxed{H_z = -E_z \sum_i T_i^z = -\tfrac{1}{2}(n_{ix} - n_{iz}),} \tag{6}$$

- **Orbital order of occupied orbitals for $i \in A, B$:**

$$\boxed{|i\mu\rangle = \cos(\frac{\pi}{4} \pm \phi)|iz\rangle + \sin(\frac{\pi}{4} \pm \phi)|ix\rangle.} \tag{7}$$

Free hole propagation and orbitons

- **The hopping H_t of spinless fermions:**

$$\boxed{\begin{aligned} H_t = \frac{1}{4}t \sum_{\langle ij\rangle} [f^\dagger_{i0}f_{j0} + f^\dagger_{i1}f_{j1} + 2(f^\dagger_{i0}f_{j1} + f^\dagger_{i1}f_{j0}) \\ + \sqrt{3}(f^\dagger_{i1}f_{j0} - f^\dagger_{i0}f_{j1}) + H.c.], \end{aligned}} \tag{8}$$

where $f^\dagger_{i\alpha}$ creates a hole in orbital $|\alpha\rangle$.

- **Orbital order tuned by E_z (uniaxial pressure):**

$$\sin 2\phi = -E_z/4J. \tag{9}$$

- **Hopping in the limit of $U \to \infty$:**

$$\boxed{H_h = \sum_{\mathbf{k}} \varepsilon^0_{\mathbf{k}}(\phi) h^\dagger_{\mathbf{k}} h_{\mathbf{k}},} \tag{10}$$

with free dispersion which vanishes at $E_z = -2J$,

$$\boxed{\varepsilon^0_{\mathbf{k}}(\phi) = t(-2\sin 2\phi + 1)\gamma_{\mathbf{k}},} \quad \gamma_{\mathbf{k}} = \frac{1}{2}(\cos k_x + \cos k_y). \tag{11}$$

- **Orbital waves:**

$$\boxed{\mathcal{H}_o = \sum_{\mathbf{k}} \omega^0_{\mathbf{k}}(\phi) \alpha^\dagger_{\mathbf{k}} \alpha_{\mathbf{k}},} \tag{12}$$

with dispersion vanishing at $E_z = \pm 2J$,

$$\boxed{\omega^0_{\mathbf{k}}(\phi) = 3J[1 + \frac{1}{3}(2\cos 4\phi - 1)\gamma_{\mathbf{k}}]^{1/2}.} \tag{13}$$

Electronic structure

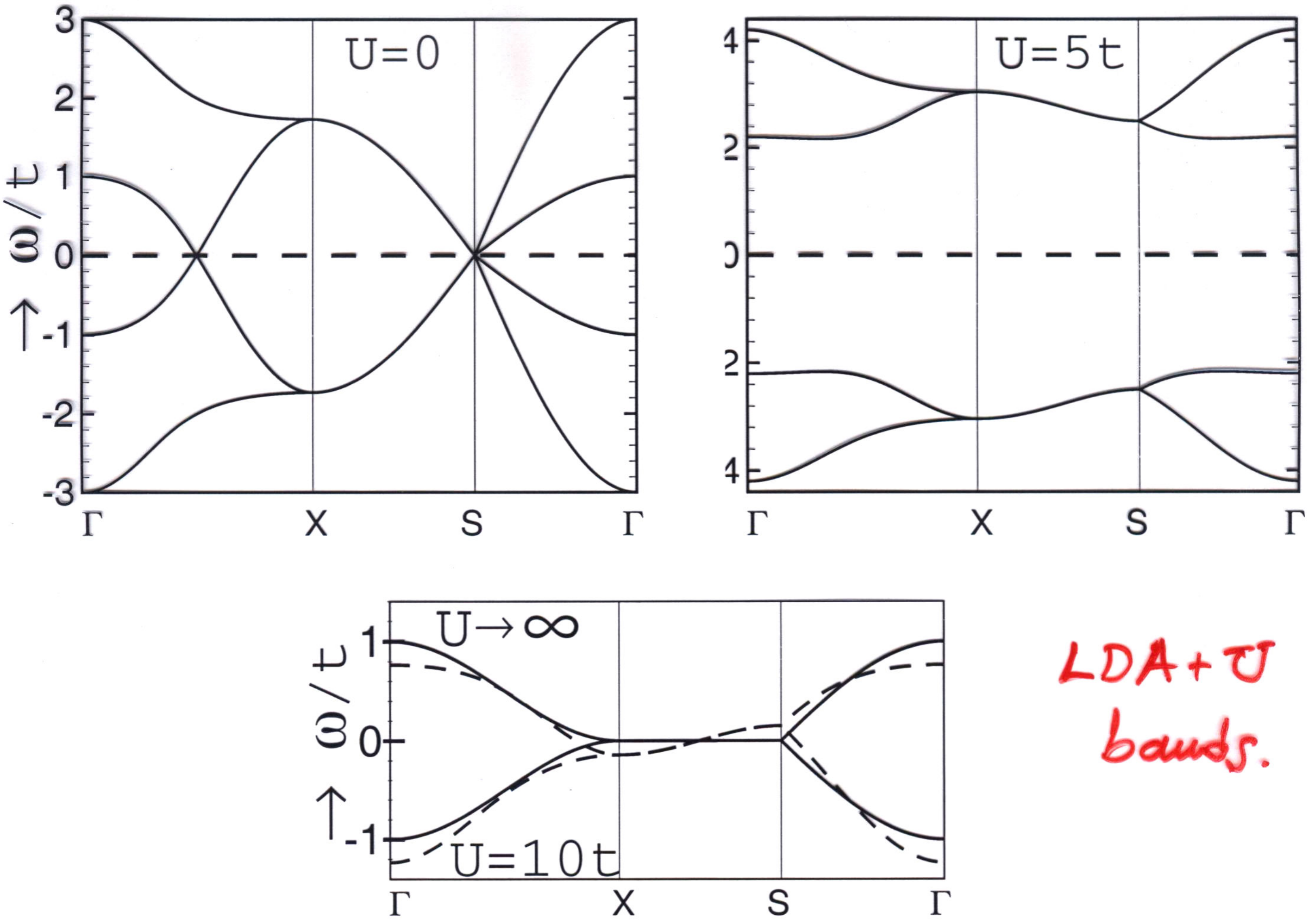

LDA+U bands.

orbital order: $(|x\rangle \pm |z\rangle)/\sqrt{2}$

Quasiparticles for $\lambda = 0$

- **Effective Hamiltonian:**

$$\mathcal{H}_{eff} = H_h + H_o + H_{ho}. \tag{14}$$

- **Hole-orbiton interaction:**

$$\boxed{\mathcal{H}_{ho} = t\sum_{\mathbf{k},\mathbf{q}} h^\dagger_{\mathbf{k}+\mathbf{q}} h_{\mathbf{k}}[M_{\mathbf{k},\mathbf{q}}\alpha_{\mathbf{q}} + N_{\mathbf{k},\mathbf{q}}\alpha_{\mathbf{q}+\mathbf{Q}} + H.c.],} \tag{15}$$

where $\mathbf{Q} = (\pi, \pi)$, and the vertex functions

$$\begin{aligned} M_{\mathbf{k},\mathbf{q}} &= 2\cos 2\phi(u_{\mathbf{q}}\gamma_{\mathbf{k}-\mathbf{q}} + v_{\mathbf{q}}\gamma_{\mathbf{k}}), \\ N_{\mathbf{k},\mathbf{q}} &= -\sqrt{3}(u_{\mathbf{q}}\eta_{\mathbf{k}-\mathbf{q}} - v_{\mathbf{q}}\eta_{\mathbf{k}}), \quad \eta_{\mathbf{k}} = \gamma_{\mathbf{k}+(0,\pi)}. \end{aligned} \tag{16}$$

- **Self-energy in SCBA:**

$$\boxed{\begin{aligned} \Sigma(\mathbf{k},\omega) = t^2[&M^2_{\mathbf{k},\mathbf{k}-\mathbf{q}} G[\mathbf{k}-\mathbf{q}, \omega - \omega_{\mathbf{q}}(\phi)] \\ &+ N^2_{\mathbf{k},\mathbf{k}-\mathbf{q}} G[\mathbf{k}-\mathbf{q}, \omega - \omega_{\mathbf{q}+\mathbf{Q}}(\phi)]], \end{aligned}} \tag{17}$$

- **Spectral function found self-consistently:**

$$A(\mathbf{k},\omega) = -\frac{1}{\pi} Im G(\mathbf{k},\omega). \tag{18}$$

- **Quasiparticles due to orbital excitations:**
  - weak intensity and large effective mass for $J/t \sim 0.1$;
  - depend on the type of occupied orbitals.

[J. van den Brink, P. Horsch, and AMO, PRL **85**, 5174]

$(|x\rangle + |z\rangle)/(|x\rangle - |z\rangle)$ $\phi = 0$

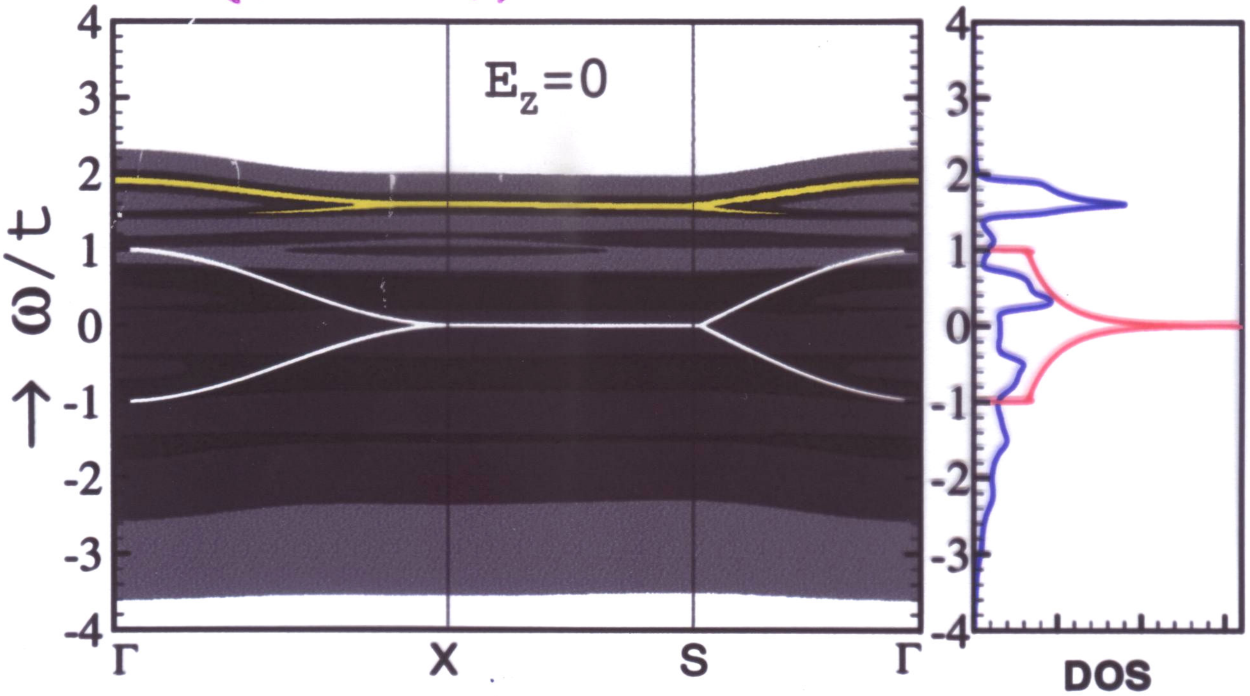

$|3x^2-r^2\rangle/|3y^2-z^2\rangle$ $\phi = -\pi/12$

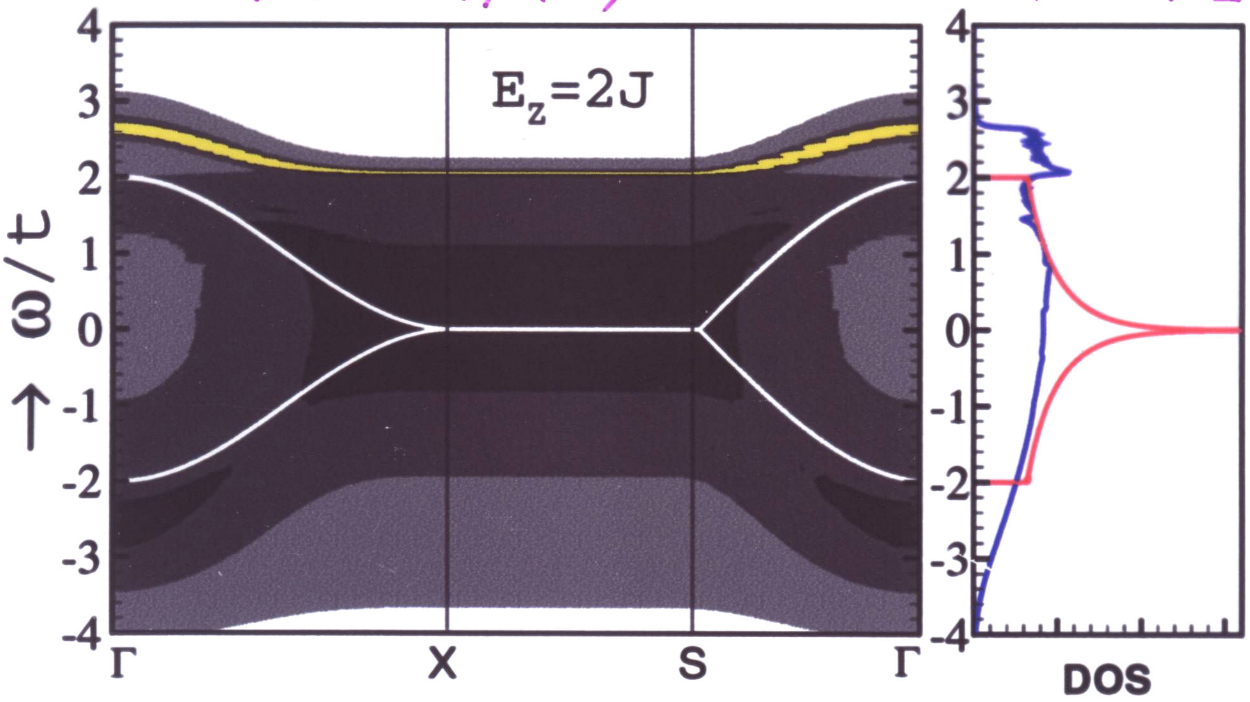

[J. van den Brink, P. Horsch, A.M. Oleś, PRL 85, 5174 (00)]

- coherent propagation at low ω
  - hole dressed by orbital excitations
- incoherent processes at high ω

Quasiparticle properties

$J/t \simeq 0.1$

$\Rightarrow W^*/W \simeq 0.1$

$\left(\frac{\partial^2 \epsilon_k}{\partial k^2}\right)\Big|_{k=0} = \frac{m}{m^*}$

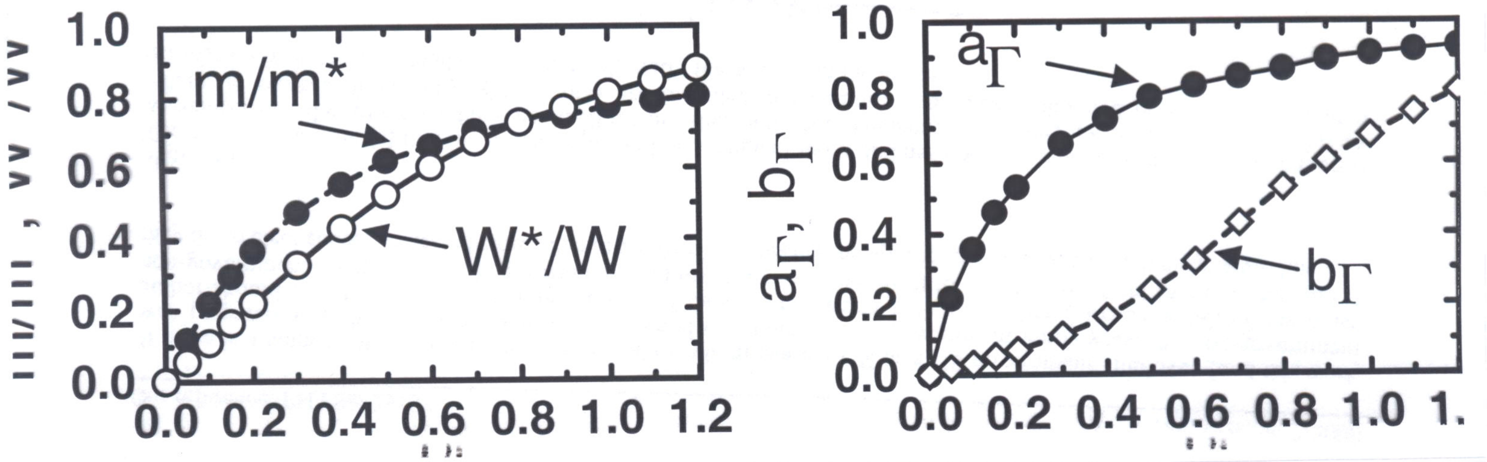

Orbital polarons in (a, b) planes of $LaMnO_3$

- **Orbitons for static Jahn-Teller effect:**

$$\boxed{\omega^0_{\mathbf{k}}(\phi) = 3J\{1 + \Lambda + [1 + \Lambda + \frac{1}{3}(2\cos 4\phi - 1)\gamma_{\mathbf{k}}]\}^{1/2},} \quad (19)$$

where the coupling constant is:

$$\Lambda = 2\lambda^2/JK. \quad (20)$$

- **Orbital polarization around a hole:**

$$\boxed{\mathcal{H}_\Delta = -\Delta \sum_\gamma \sum_{\langle ij \rangle} n_i \tau^\gamma_j,} \quad (21)$$

with $\tau^{a(b)}_j = \frac{1}{2}(T^z_i \mp \sqrt{3} T^x_i)$, $\tau^c_j = T^z_i$, $n_i = h^\dagger_i h_i$.

– favors orbitals directed towards the hole,

– gives additional hole scattering.

[R. Kilian and G. Khaliullin, PRB **60**, 13458 (1999)]

- **Quasiparticle dispersion:**

– increases with increasing λ;

– decreases with increasing Δ.

[J. Bała, AMO, P. Horsch, PRB **60**, 134420 (2002)]

Spectral function $A(k,\omega)$

$\lambda = 10t, \quad \Delta = 0.75t$

$J/t = 0.1$

QP band minimum

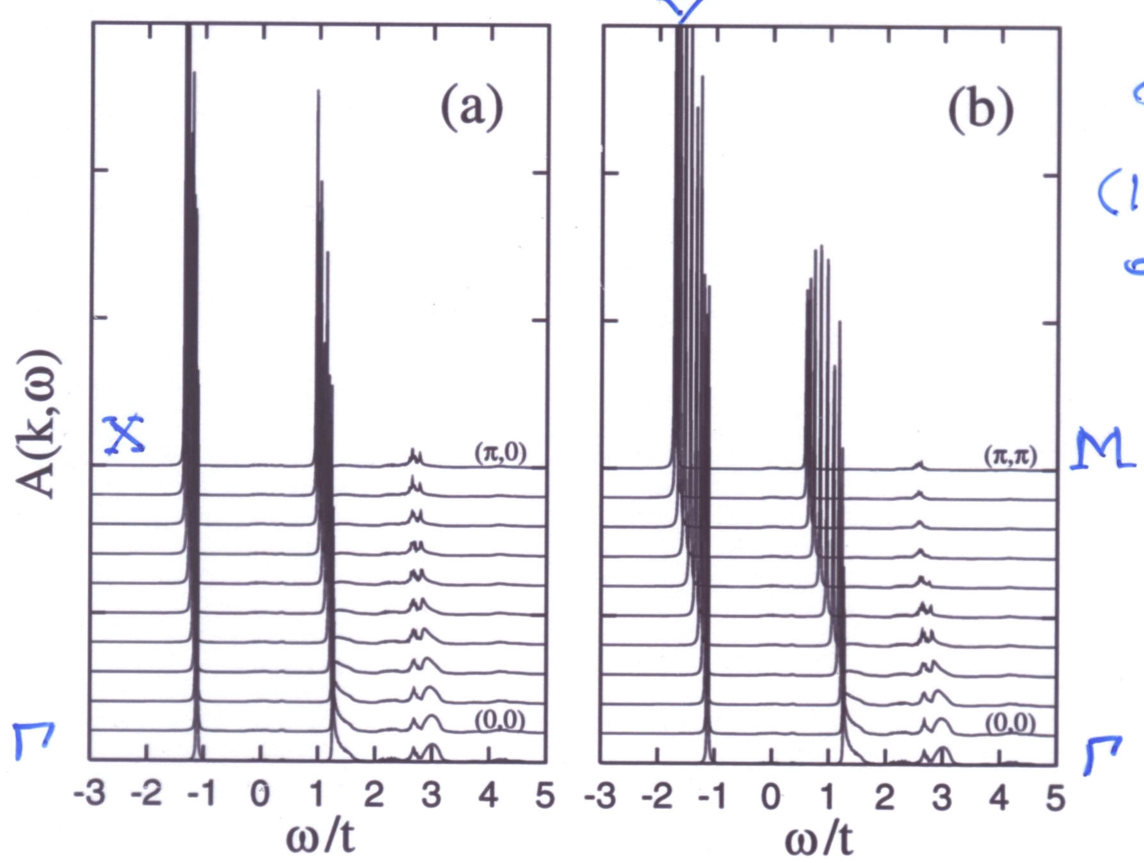

$\phi = 0$

$(|x\rangle \pm |z\rangle)$ orbitals

[J. Bala et al., PRB 65, 134420 (02)]

Fig. 4

Hole spectral functions

$J=0.1t$, $\lambda=10t$, $\Delta=0.75t$

$\phi=-\pi/12$

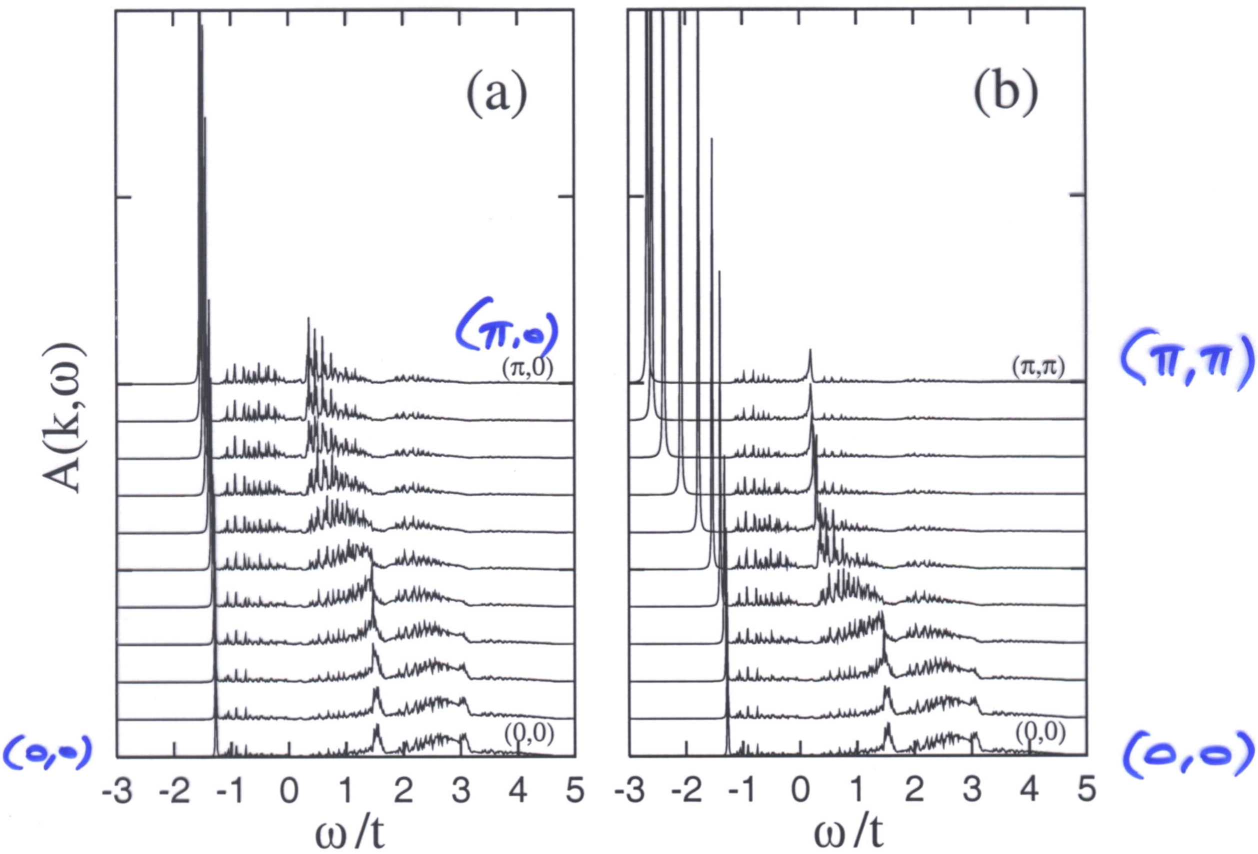

Fig. 5

Hole spectral functions

J=0.1t, λ=0

Δ=0 Δ=t

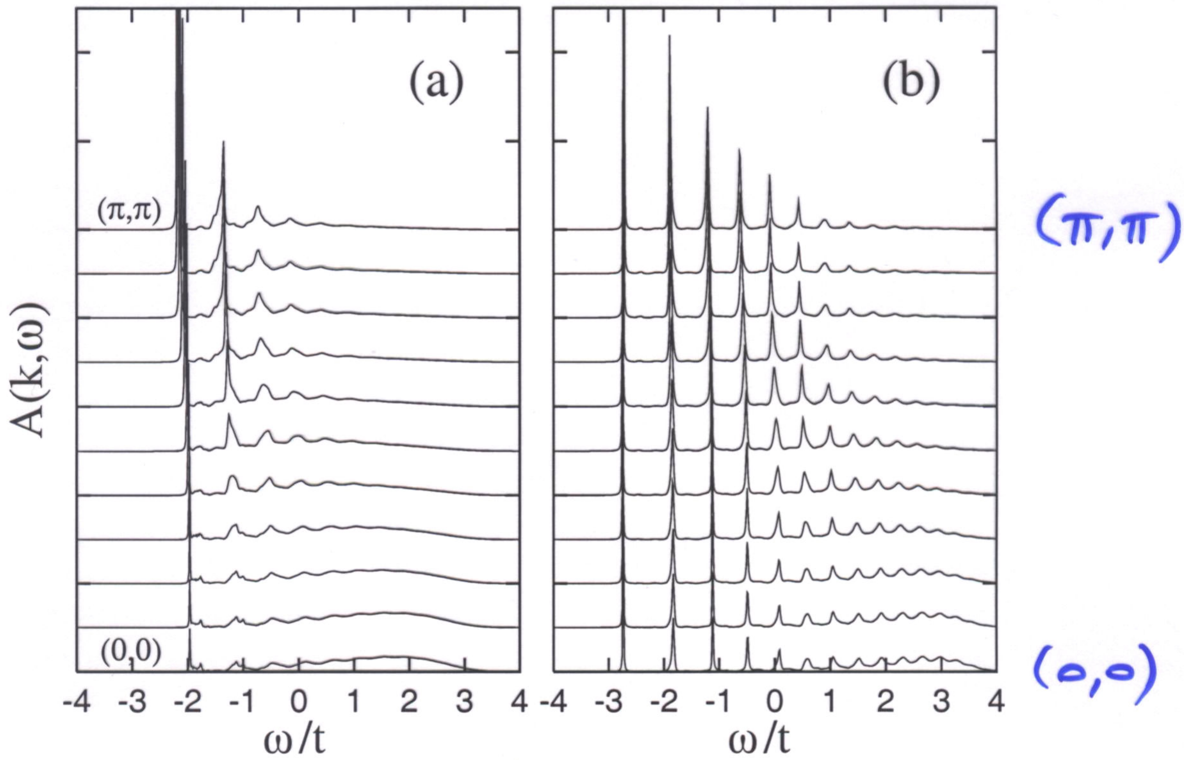

Fig. 7

Quasiparticle dispersion

$J/t = 0.1$

$\phi = 0$

$\Delta = 0,\ \lambda = 10t$

$\Delta = t,\ \lambda = 10t$

$\Delta = \lambda = 0$

$\Delta = t,\ \lambda = 0$

$\phi = -\pi/12$

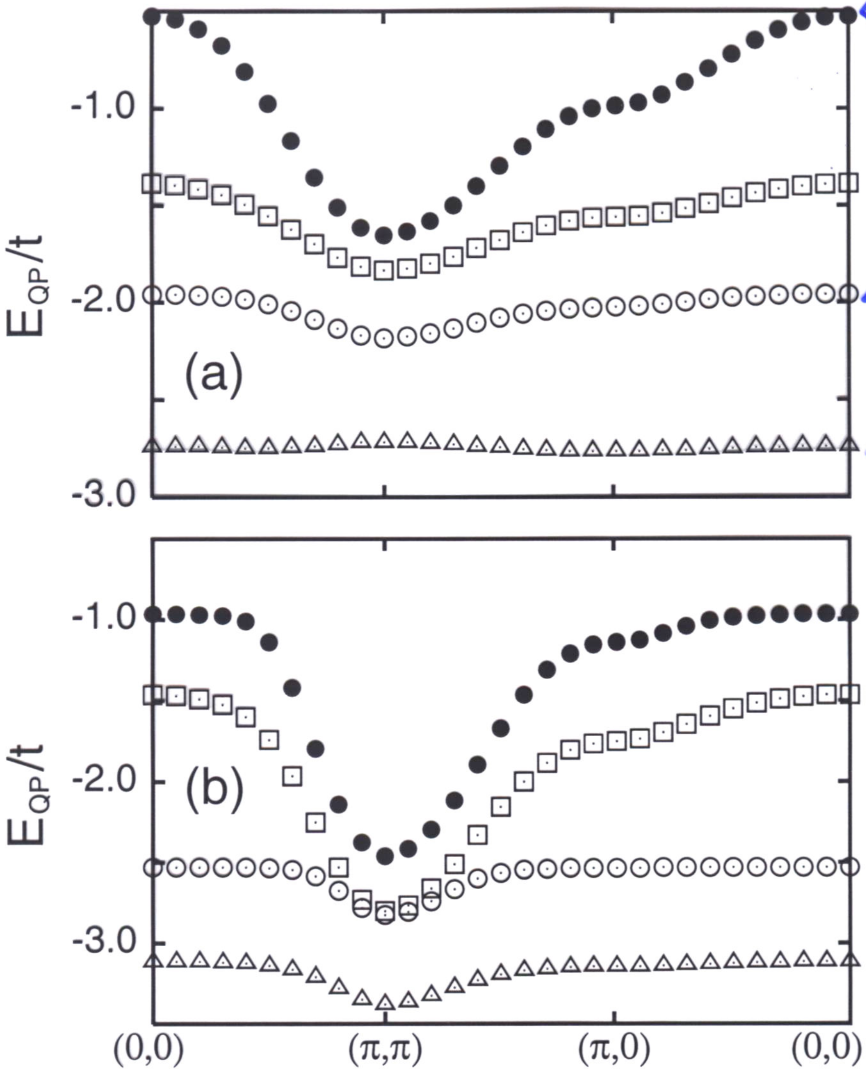

Fig. 8

Orbital-lattice polarons

- **Effective hole-orbiton-phonon problem:**

$$
\boxed{\begin{aligned}
\mathcal{H}_{eff} = &\sum_{\mathbf{k}} \varepsilon_{\mathbf{k}}(\phi) h_{\mathbf{k}}^{\dagger} h_{\mathbf{k}} + \sum_{\mathbf{q}} \sum_{\xi=1,2} \Omega_{\mathbf{q}}^{(\xi)}(\phi) \beta_{\mathbf{q},\xi}^{\dagger} \beta_{\mathbf{q},\xi} \\
&+ \omega_0 \sum_{\mathbf{q},\mu=1,3} B_{\mathbf{q},\mu}^{\dagger} B_{\mathbf{q},\mu} \\
&+ \sum_{\mathbf{k},\mathbf{q}} \{ h_{\mathbf{k}-\mathbf{q}}^{\dagger} h_{\mathbf{k}} [M_0 \left(\sqrt{2} B_{\mathbf{q},1}^{\dagger} + B_{\mathbf{q},3}^{\dagger} \right) \\
&\qquad + \sum_{\xi=1,2} \left(M_{\mathbf{k},\mathbf{q}}^{(\xi)} \beta_{\mathbf{q},\xi}^{\dagger} + N_{\mathbf{k},\mathbf{q}}^{(\xi)} \beta_{\mathbf{q}+\mathbf{Q},\xi}^{\dagger} \right)] + \text{H.c.} \},
\end{aligned}} \quad (22)
$$

with the phonon mode $\omega_0 = \sqrt{2K/M}$ and the hole-phonon vertex $M_0 = \sqrt{3/N}\lambda/(2KM)^{1/4}$.

- **Mixed orbiton-phonon modes:**
  $\Omega_{\mathbf{q}}^{(\xi)}(\phi)$ are mixed electron-phonon excitations
  $M_{\mathbf{k},\mathbf{q}}^{(\xi)}$ are the respective vertices.
- **Phonon softening for large JT coupling**
- **Broad quasiparticles (vibrational side bands)**
  [J. Bała, AMO, G.A. Sawatzky, PRB **65**, 184414 (2002)]

Mixed exiton-phonon excitations

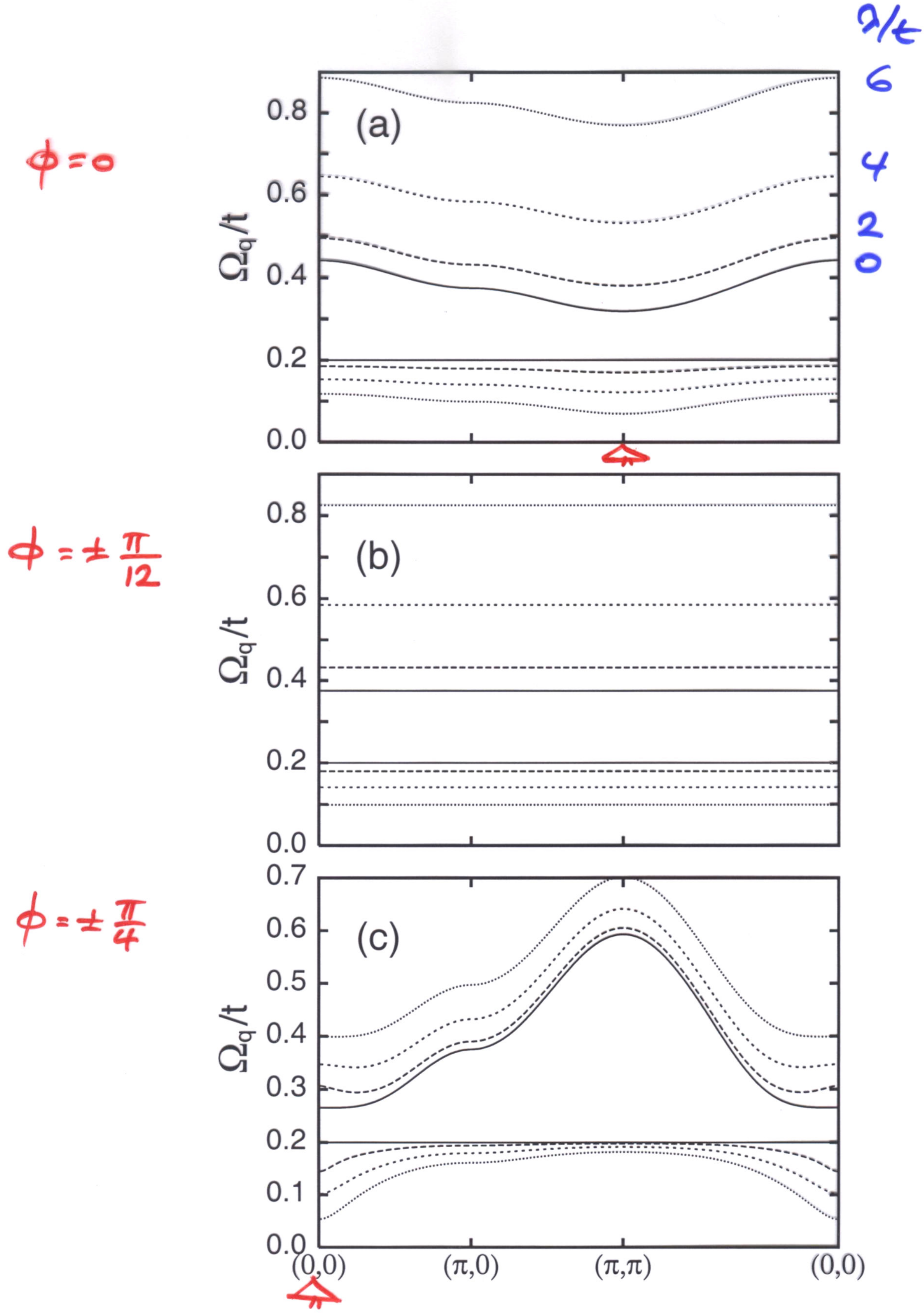

Fig. 1

Local hole spectral functions

$|x^2-z^2\rangle / |y^2-z^2\rangle$ order

$J/t = 1/8$

$\lambda/t=0$

$\lambda/t=4$

$\lambda/t=8$

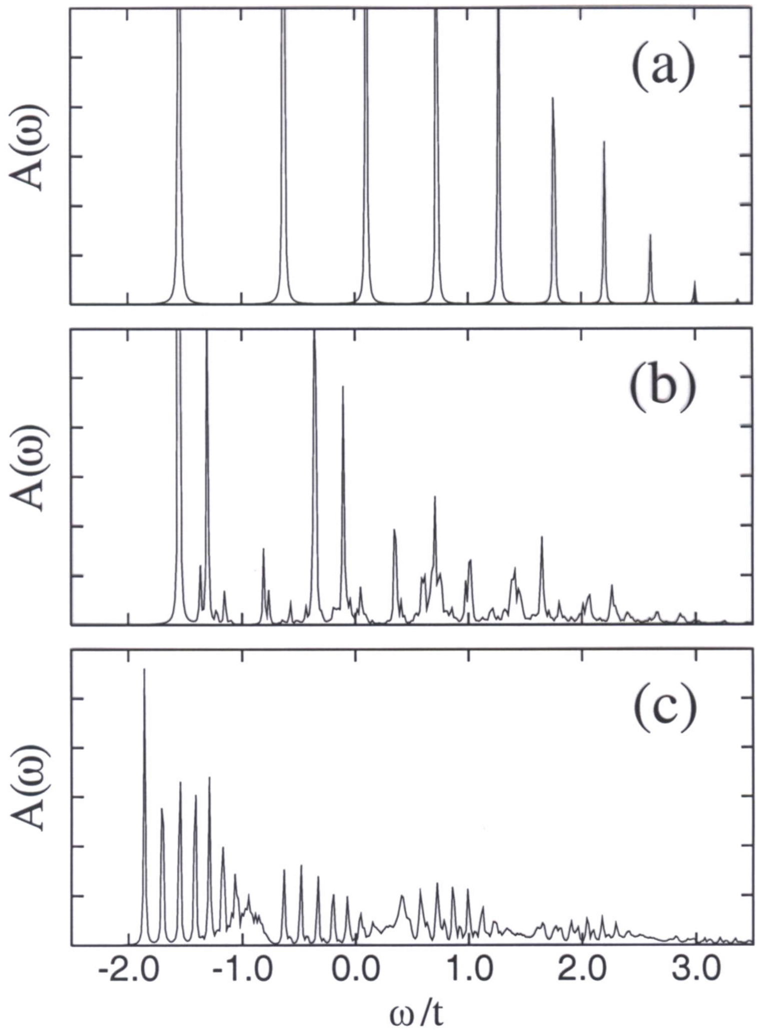

Fig. 3

Quantum decoherence in A-AF phase

- **Effective Hamiltonian:**

$$\mathcal{H}_{eff} = H_t + H_J. \tag{23}$$

- **Hopping in the orbital ordered state:**

$$\boxed{H_t = t^{\phi}_{ab} \sum_{\langle ij\rangle_{ab},\sigma} \tilde{c}^{\dagger}_{i\sigma}\tilde{c}_{j\sigma} - t^{\phi}_{c} \sum_{\langle ij\rangle_{c},\sigma} \tilde{c}^{\dagger}_{i\sigma}\tilde{c}_{j\sigma} + \mathrm{H.c.},} \tag{24}$$

with $t^{\phi}_{ab} = \frac{1}{4}t\,[1 - 2\sin(2\phi)]$ and $t^{\phi}_{c} = \frac{1}{2}t\,[1 + \sin(2\phi)]$.

- **Magnons in A-AF phase:**

$$\omega_{\mathbf{q}} = \{A^2_{\mathbf{q}} - B^2_{\mathbf{q}}\}^{1/2}, \tag{25}$$

where $A_{\mathbf{q}} = 2S[J_c + 2J_{ab}(1 - \gamma^{\parallel}_{\mathbf{q}})]$, $B_{\mathbf{q}} = 2SJ_c\gamma^{z}_{\mathbf{q}}$,

- **Hole-magnon effective Hamiltonian:**

$$\boxed{\begin{aligned}\mathcal{H}_{\mathrm{LSW}} &= \sum_{\mathbf{k}} \varepsilon_{\mathbf{k}}(\phi) h^{\dagger}_{\mathbf{k}} h_{\mathbf{k}} + \sum_{\mathbf{q}} \omega_{\mathbf{q}} \beta^{\dagger}_{\mathbf{q}} \beta_{\mathbf{q}} \\ &+ \frac{1}{\sqrt{N}} \sum_{\mathbf{k},\mathbf{q}} \left[M_{\mathbf{k},\mathbf{q}}(\phi) h^{\dagger}_{\mathbf{k}} h_{\mathbf{k}-\mathbf{q}} \beta_{\mathbf{q}} + \mathrm{H.c.} \right],\end{aligned}} \tag{26}$$

$$\boxed{M_{\mathbf{k},\mathbf{q}}(\phi) = t^{\phi}_{c}(\gamma^{z}_{\mathbf{k}-\mathbf{q}} u_{\mathbf{q}} + \gamma^{z}_{\mathbf{k}} v_{\mathbf{q}}).} \tag{27}$$

- **Self-energy in SCBA:**

$$\boxed{\Sigma(\mathbf{k},\omega) = \frac{1}{N} \sum_{\mathbf{q}} M^2_{\mathbf{k},\mathbf{q}}(\phi) G(\mathbf{k}-\mathbf{q}, \omega - \omega_{\mathbf{q}}).} \tag{28}$$

- **Incoherent proceses dominate for large** $t^{\phi}_{c}/t^{\phi}_{ab}$

[J. Bała *et al.*, PRL **87**, 067204 (2001)]

Hole spectral functions

$\phi = \pi/24\,,\quad t_c^{\phi}/t_{ab}^{\phi} = 5.2$

$|E_{QP}(\pi,\pi,0) - E(0,0,\pi/2)| \sim 2J$

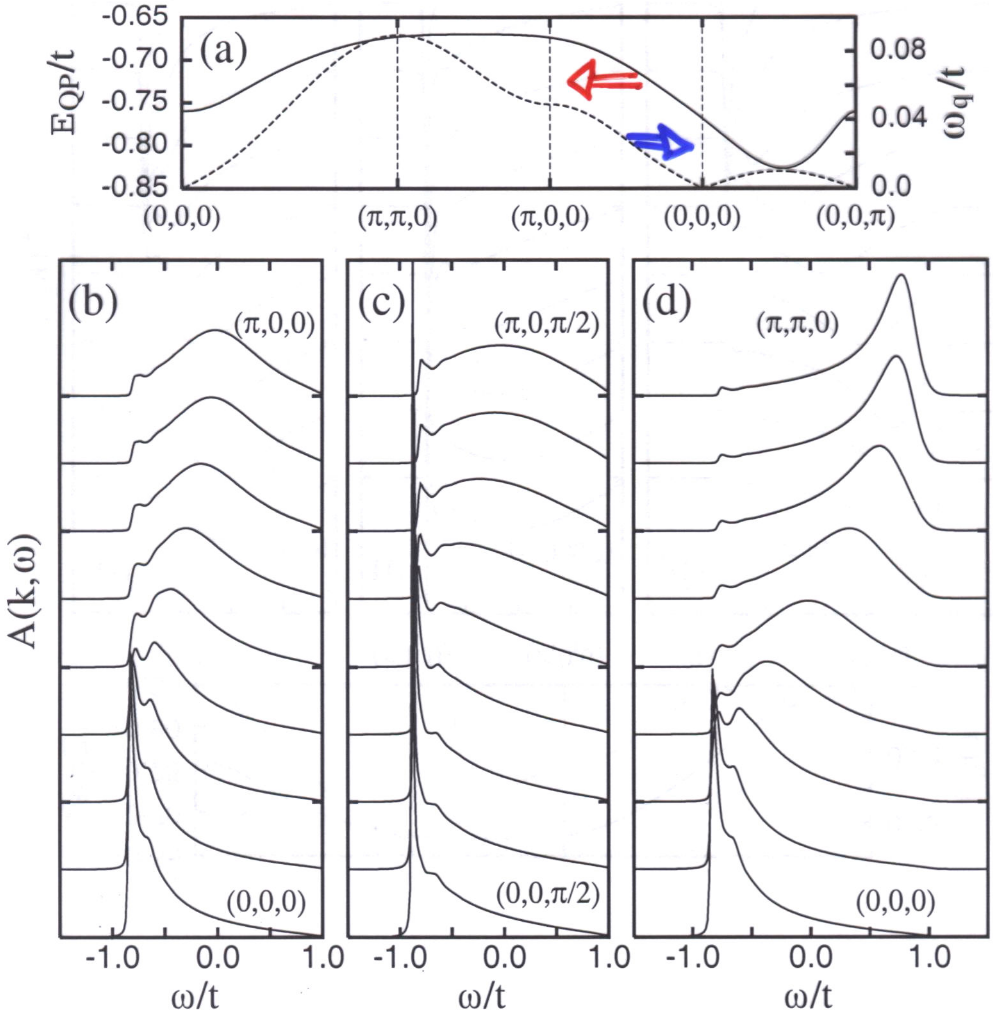

Magnon

Fig. 4

CE phase

$La_{1/2}Sr_{3/2}MnO_4$

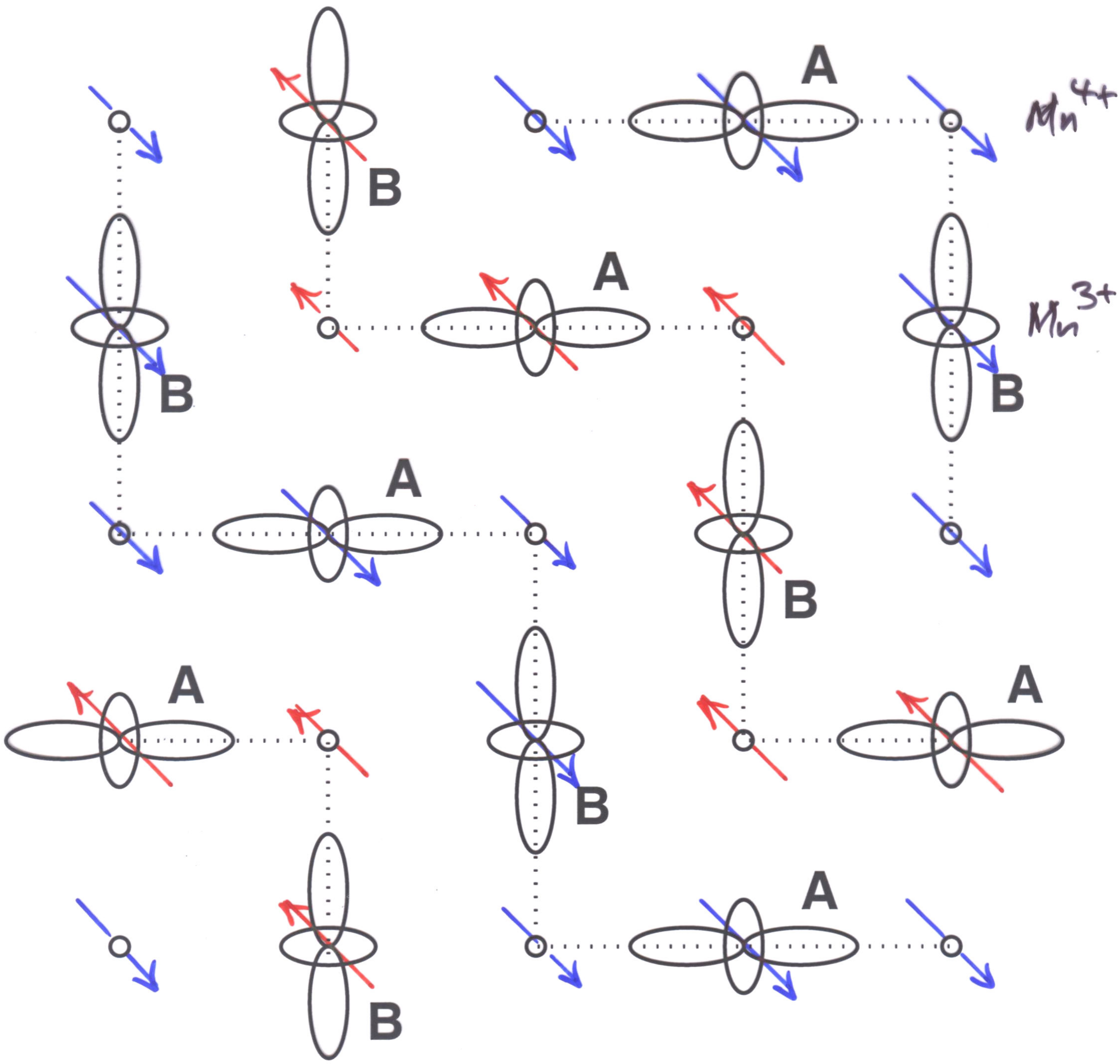

Spectral functions for CE phase, $T < T_N$

$\phi = -\pi/12$

weak coupling

$\lambda = 10t$

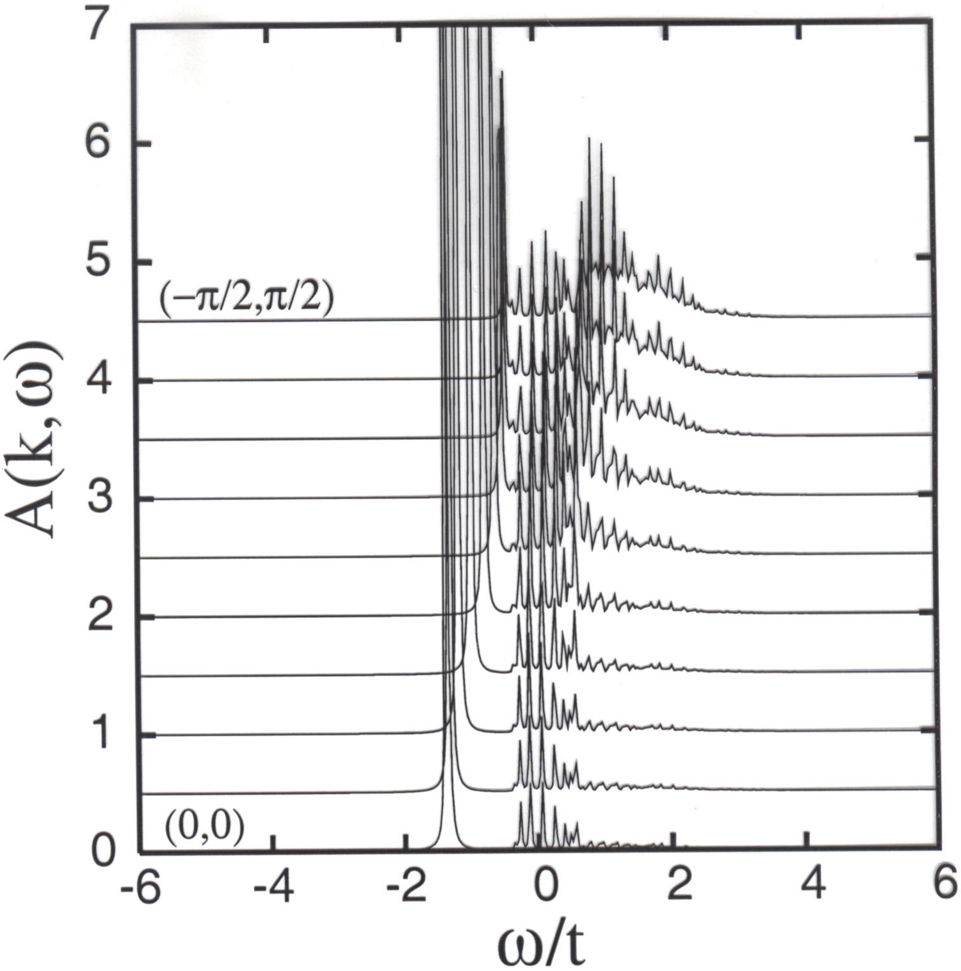

Strong coupling

$\lambda = 40t$

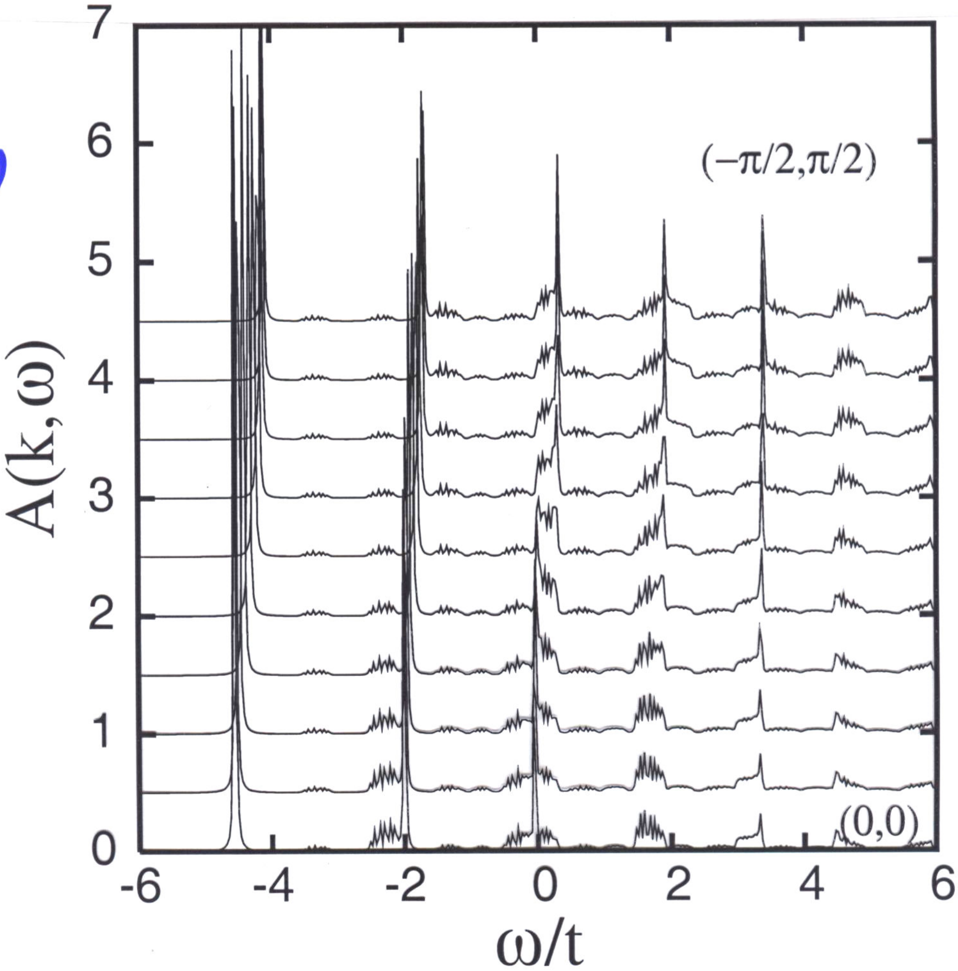

Orbital t-J Model in 1D ($T = 0$)

- **We consider the 1D orbital t-J model:**

$$\mathcal{H}_0 = H_t + H_J + H_{\rm JT}, \tag{29}$$

for e_g electrons in FM manganites at $T = 0$. We use the orbital basis $\{x^2 - y^2, 3z^2 - r^2\}$ for a chain along c axis:

$$|x\rangle \equiv \tfrac{1}{\sqrt{2}}|x^2 - y^2\rangle, \quad |z\rangle \equiv \tfrac{1}{\sqrt{6}}|3z^2 - r^2\rangle. \tag{30}$$

- **The hopping H_t of spinless fermions:**

$$\boxed{H_t = -t\sum_i(\tilde{c}^\dagger_{iz}\tilde{c}_{i+1,z} + \tilde{c}^\dagger_{i+1,z}\tilde{c}_{iz}),} \tag{31}$$

where $\tilde{c}^\dagger_{iz} = c^\dagger_{iz}(1 - n_{ix})$ creates a $|z\rangle$ electron at empty site.

- **The orbital superexchange (classical):**

$$\boxed{H_J = 2J\sum_i(T^z_i T^z_{i+1} - \tfrac{1}{4}\tilde{n}_i\tilde{n}_{i+1}),} \tag{32}$$

$$T^z_i = \tfrac{1}{2}\sigma^z_i = \tfrac{1}{2}(n_{ix} - n_{iz}). \tag{33}$$

- **The cooperative JT effect:**

$$\boxed{H_{\rm JT} = 2E_{\rm JT}\sum_i \exp(i\pi R_i)T^z_i,} \tag{34}$$

supports alternating orbitals (energy gain $E_{\rm JT}$ per site).

- **Spin 1D t-J model (quantum):**

$$\boxed{\begin{aligned}\mathcal{H}_{tJ} = &-t\sum_{i\sigma}(\tilde{c}^\dagger_{i\sigma}\tilde{c}_{i+1,\sigma} + \tilde{c}^\dagger_{i+1,\sigma}\tilde{c}_{i\sigma}) \\ &+ 2J\sum_i \vec{S}_i\cdot\vec{S}_{i+1} + 2h_s\sum_i \exp(i\pi R_i)S^z_i.\end{aligned}} \tag{35}$$

Orbital t-J Model in 1D ($T=0$)

- **We consider the 1D orbital t-J model:**

$$\mathcal{H}_0 = H_t + H_J + H_{\rm JT}, \tag{29}$$

for e_g electrons in FM manganites at $T=0$. We use the orbital basis $\{x^2-y^2, 3z^2-r^2\}$ for a chain along c axis:

$$|x\rangle \equiv \tfrac{1}{\sqrt{2}}|x^2-y^2\rangle, \quad |z\rangle \equiv \tfrac{1}{\sqrt{6}}|3z^2-r^2\rangle. \tag{30}$$

- **The hopping H_t of spinless fermions:**

$$\boxed{H_t = -t\sum_i(\tilde{c}^\dagger_{iz}\tilde{c}_{i+1,z} + \tilde{c}^\dagger_{i+1,z}\tilde{c}_{iz}),} \tag{31}$$

where $\tilde{c}^\dagger_{iz} = c^\dagger_{iz}(1-n_{ix})$ creates a $|z\rangle$ electron at empty site.

- **The orbital superexchange (classical):**

$$\boxed{H_J = 2J\sum_i\left(T^z_iT^z_{i+1} - \tfrac{1}{4}\tilde{n}_i\tilde{n}_{i+1}\right),} \tag{32}$$

$$T^z_i = \tfrac{1}{2}\sigma^z_i = \tfrac{1}{2}(n_{ix}-n_{iz}). \tag{33}$$

- **The cooperative JT effect:**

$$\boxed{H_{\rm JT} = 2E_{\rm JT}\sum_i \exp(i\pi R_i)T^z_i,} \tag{34}$$

supports alternating orbitals (energy gain $E_{\rm JT}$ per site).

- **Spin 1D t-J model (quantum):**

$$\boxed{\begin{aligned}\mathcal{H}_{tJ} = &-t\sum_{i\sigma}(\tilde{c}^\dagger_{i\sigma}\tilde{c}_{i+1,\sigma} + \tilde{c}^\dagger_{i+1,\sigma}\tilde{c}_{i\sigma}) \\ &+ 2J\sum_i \vec{S}_i\cdot\vec{S}_{i+1} + 2h_s\sum_i\exp(i\pi R_i)S^z_i.\end{aligned}} \tag{35}$$

Hole in AO and FO states

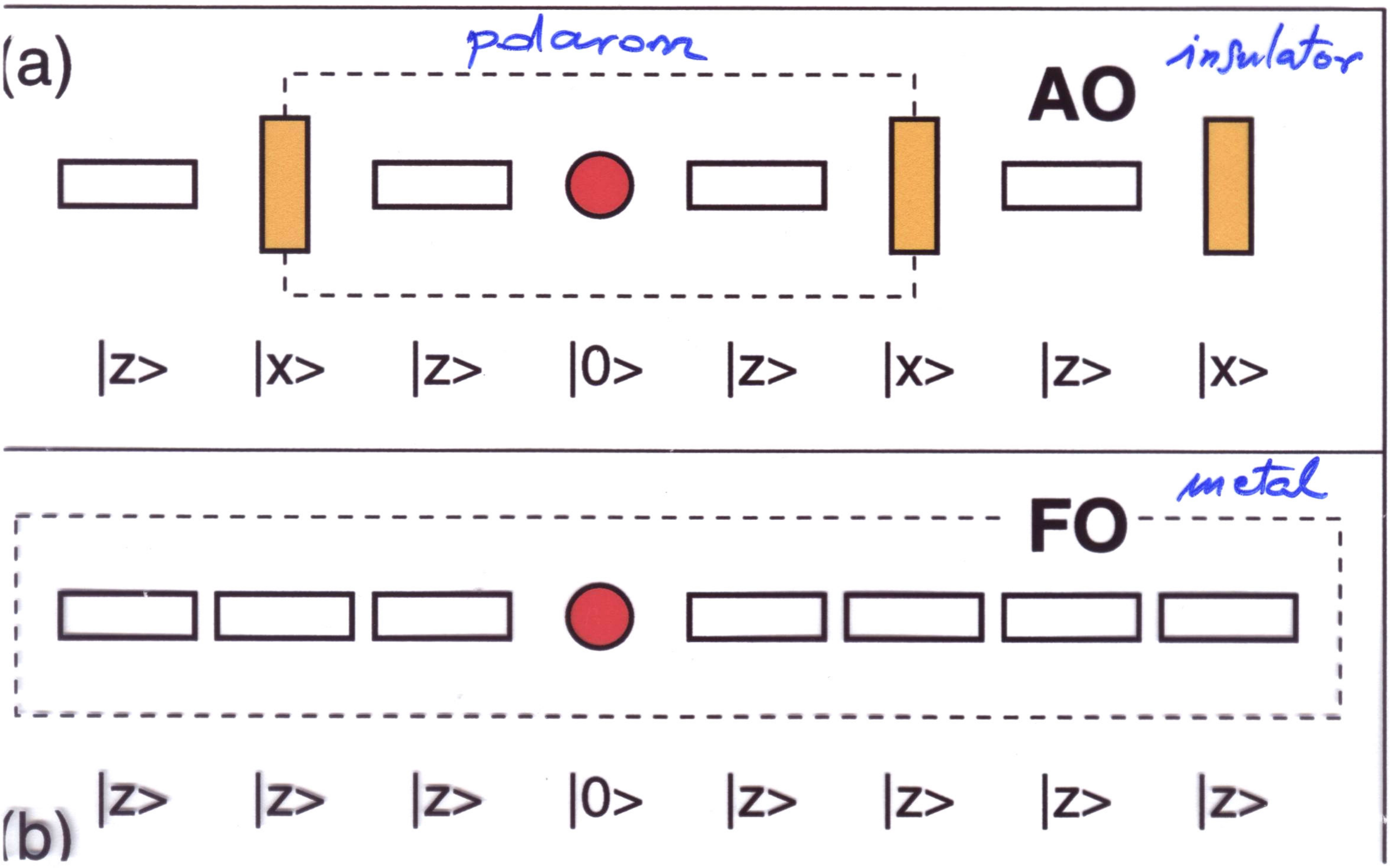

Spectral functions

$J = 0.125t, \quad J' = 0.02t, \quad E_{JT} = 0.25t$

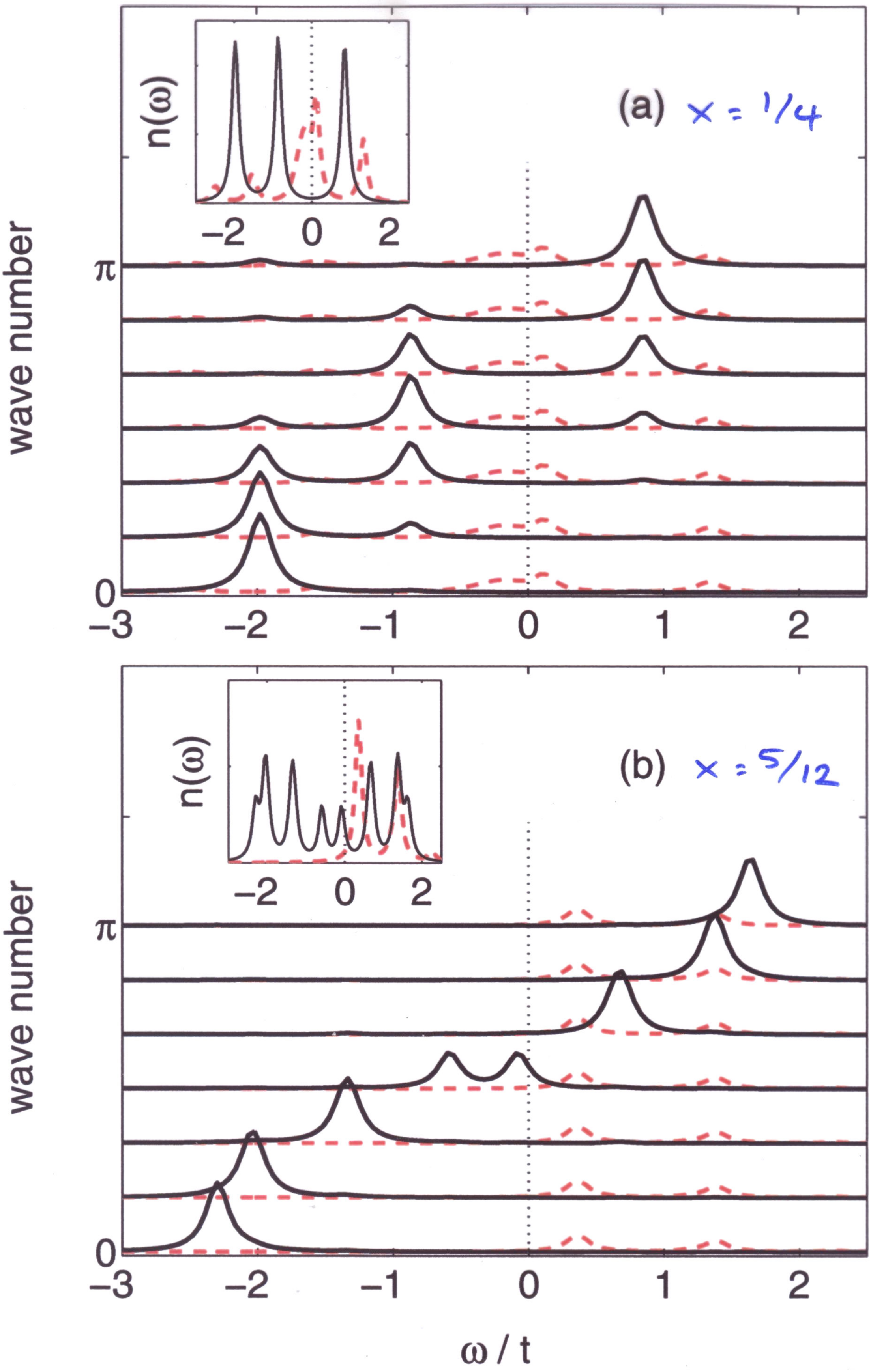

1D orbital t-J model at finite T

- **Full Hamiltonian:**

$$\mathcal{H}(\mathcal{S}) = H_t + H_J + H_{J'} + H_{\rm JT}, \tag{36}$$

- **Effective orbital t-J model $\mathcal{H}(\mathcal{S})$ at $T > 0$:**

$$\boxed{\begin{aligned} H_t &= -\sum_i \tilde{t}_{i,i+1}(\tilde{c}^\dagger_{iz}\tilde{c}_{i+1,z} + \tilde{c}^\dagger_{i+1,z}\tilde{c}_{iz}), & (37)\\ H_J &= \frac{1}{5}J\sum_i (2u^2_{i,i+1}+3)(2T^z_iT^z_{i+1} - \tfrac{1}{2}\tilde{n}_i\tilde{n}_{i+1}) & \\ &- \frac{9}{10}J\sum_i(1-u^2_{i,i+1})\tilde{n}_{iz}\tilde{n}_{i+1,z} & (38)\\ &- J\sum_i(1-u^2_{i,i+1})[\tilde{n}_{iz}(1-\tilde{n}_{i+1}) + (1-\tilde{n}_i)\tilde{n}_{i+1,z}]. & \end{aligned}}$$

[from L.F. Feiner and A.M. Oleś, PRB **59**, 3295 (1999)]

- **Superexchange for t_{2g} spins:**

$$\boxed{H_{J'} = J'\sum_i(\vec{S}_i\cdot\vec{S}_{i+1} - S^2).} \tag{39}$$

$$\boxed{\langle\vec{S}_i\cdot\vec{S}_{i+1}\rangle = S^2(2u^2_{i,i+1}-1),} \tag{40}$$

where $u_{i,i+1} = \cos(\theta_{i,i+1}/2)e^{i\chi_{i,j}}$, and directions of two classical spins at sites i and $i+1$ differ by $\theta_{i,i+1}$.

- **The cooperative JT effect:**

$$\boxed{H_{\rm JT} = 2E_{\rm JT}\sum_i \exp(i\pi R_i)T^z_i,} \tag{41}$$

- **Monte Carlo treatment of t_{2g} spins**
- **Doping: from localized to itinerant spectra**
  [M. Daghofer, AMO, W. von den Linden, PRB **70**, 184430]

Spectral functions

$J/t = 0.125$, $J' = 0.02t$, $E_{JT} = 0$

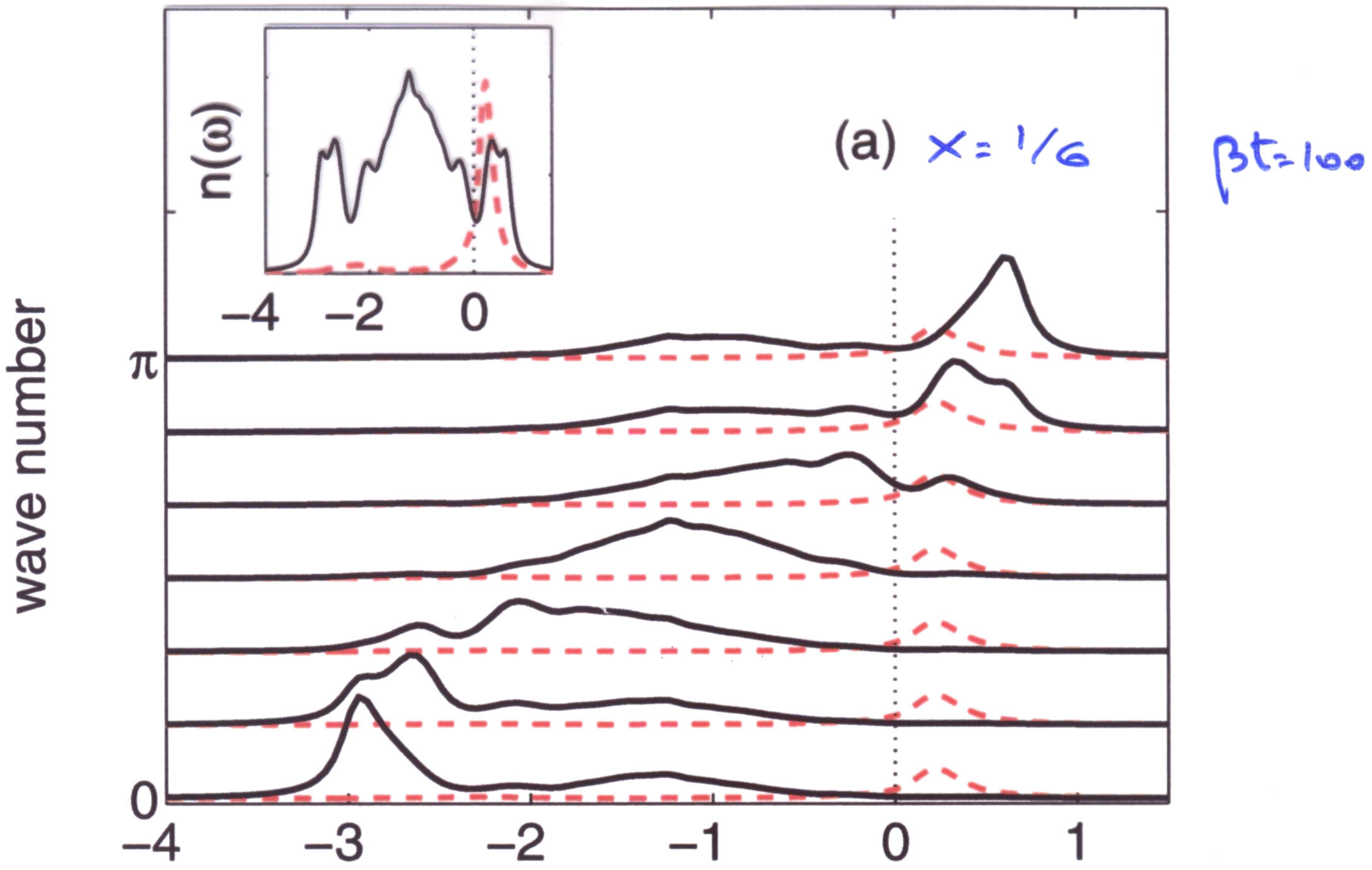

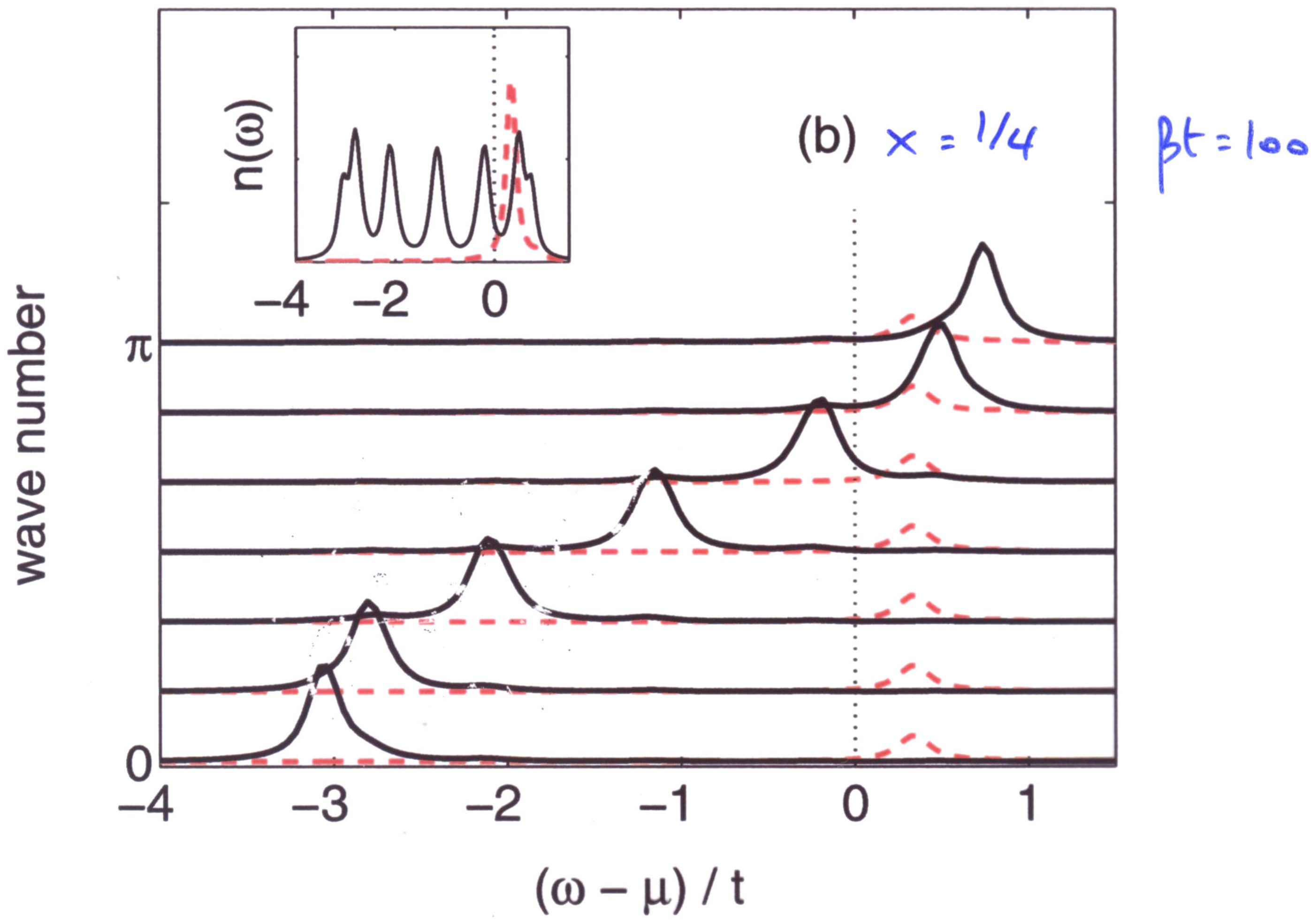

Parameters and double exchange

- **Two parameters: J/t and E_{JT}/t.**
- **Experimental input:**

$$t \simeq 0.4 - 0.5 \ \text{eV}, \tag{42}$$

$$\varepsilon(^6A_1) = U - 3J_H \simeq 3.8 \ \text{eV}, \tag{43}$$

$$=> J \simeq 0.125t \tag{44}$$

From the value of $T_N \simeq 110$ K in $\mathrm{CaMnO_3}$:

$$J' \simeq 0.004t \tag{45}$$

- **Estimation of double exchange interaction:**

$$H_s = -J_{\mathrm{DE}} \sum_{\langle ij \rangle} \vec{S}_i \cdot \vec{S}_j, \tag{46}$$

Double exchange constant is given by the kinetic energy,

$$\boxed{J_{\mathrm{DE}} = \frac{|\langle H_t \rangle|}{2zS^2},} \tag{47}$$

with $z = 2$ and $S = (4 - x)/2$.

$$x = 0.25\text{:} \ J_{\mathrm{DE}} \simeq 0.030, 0.027, 0.024t$$
$$\text{for } E_{\mathrm{JT}} = 0, 0.1 \text{ and } 0.25t$$
$$x = 0.42\text{:} \ J_{\mathrm{DE}} \simeq 0.046t$$
$$\text{for } E_{\mathrm{JT}} \leq 0.25t \text{ (metallic phase)}$$

Search for quasiparticles in manganites

1. **Orbital t-J model:**
   - far richer than the spin t-J model;
   - mixed orbiton-phonon excitations;
   - spectra depend on J/t, λ and orbital order ϕ.
2. **Quasiparticle minimum at:**
   - $\mathbf{k} = (\pi, \pi, k_z)$ for hole-orbiton scattering;
   - $\mathbf{k} = (0, 0, \pi/2)$ for hole-magnon scattering.
3. **Generic features even in the 1D model**:
   - crossover from AF insulator to FM metal with x
   - from quasiparticles to metallic spectral functions.

ARPES experiments could help to establish
- **type of quasiparticle states in manganites**
- **changes in the orbital order under doping**

Acknowledgments

for all (present and absent) participants to:

Jörg Fink
Konrad Matho
Erwin Müller-Hartmann

for organizing this nice **ARPES Workshop** —

$\boxed{\text{Thank you!}}$